remote sensing

MDPI

Article

Spatial–Temporal Assessment of Eco-Environment Quality with a New Comprehensive Remote Sensing Ecological Index (CRSEI) Based on Quaternion Copula Function

Zongmin Wang [1], Longfei Hou [1], Haibo Yang [1,*], Yong Zhao [2], Fei Chen [3], Qizhao Li [1] and Zheng Duan [4]

[1] School of Water Conservancy and Transportation, Zhengzhou University, Zhengzhou 450001, China; zmwang@zzu.edu.cn (Z.W.); houlf@gs.zzu.edu.cn (L.H.); lijun201127@gs.zzu.edu.cn (Q.L.)
[2] China Institute of Water Resources and Hydropower Research, Beijing 100038, China; zhaoyong@iwhr.com
[3] General Institute of Water Conservancy and Hydropower Planning and Design, Ministry of Water Resources of China, Beijing 100120, China; chenfei@giwp.org.cn
[4] Department of Physical Geography and Ecosystem Science, Lund University, S-22362 Lund, Sweden; zheng.duan@nateko.lu.se
* Correspondence: yanghb@zzu.edu.cn

Abstract: The traditional remote sensing ecological index (RSEI), based on principal component analysis (PCA) to integrate four evaluation indexes: greenness (NDVI), humidity (WET), dryness (NDBSI), and heat (LST), is insufficient to comprehensively consider the influence of each eco-environment evaluation index on eco-environment quality (EEQ). In this research, a new comprehensive remote sensing ecological index (CRSEI) based on the quaternion Copula function is proposed to comprehensively characterize EEQ responded by integrating four eco-environment evaluation indexes. Additionally, the spatiotemporal variation of EEQ in Henan Province is evaluated using monthly CRSEI data from 2001 to 2020. The results show that: (1) The applicability and monitoring accuracy of CRSEI are better than that of RSEI, which can be used to assess the EEQ. (2) The EEQ of Henan Province declined between 2001 and 2010 but significantly improved and rebounded from 2011 to 2020. During this period, CRSEI values were higher in West and South Henan and lowest in central Henan, with West Henan consistently showing the highest values across all seasons. (3) The EEQ in Henan Province exhibited a tendency of deterioration from the central cities outward, followed by improvement from the outer areas back towards the central cities. In 2010, regions with poor EEQ made up 68.3% of the total area, whereas by 2020, regions with excellent EEQ accounted for 74% of the total area. (4) The EEQ was significantly negatively correlated with human activities, while it was positively correlated with precipitation. The research provides a reference and guidance for the scientific assessment of the regional eco-environment.

Keywords: remote sensing ecological index; quaternion copula function; spatial–temporal changes; eco-environment quality

Citation: Wang, Z.; Hou, L.; Yang, H.; Zhao, Y.; Chen, F.; Li, Q.; Duan, Z. Spatial–Temporal Assessment of Eco-Environment Quality with a New Comprehensive Remote Sensing Ecological Index (CRSEI) Based on Quaternion Copula Function. *Remote Sens.* **2024**, *16*, 3580. https://doi.org/10.3390/rs16193580

Academic Editors: Emanuele Mandanici and Sara Kasmaeeyazdi

Received: 19 August 2024
Revised: 21 September 2024
Accepted: 23 September 2024
Published: 26 September 2024

1. Introduction

Nowadays, global ecosystems are encountering various problems due to human disturbance and accompanying environmental changes [1]. Eco-environment changes caused by human activities vary in their expression concerning distance, magnitude, and duration [2]. The eco-environment quality (EEQ) can accurately express the response relationship between regional environment and human activities [3]. Therefore, there is an increasing need for dependable models and specifications to scientifically evaluate the status of EEQ.

Recently, the research on regional EEQ can be categorized into two main approaches: (1) Evaluation of EEQ using individual indicators, such as using the normalized vegetation index (NDVI) [4–6], leaf area index (LAI) [7,8], and enhanced vegetation index (EVI) [9].

The land surface temperature index (LST) of remote sensing (RS) thermal imaging was used to evaluate the urban heat island effect [10–13], as well as the use of drought indices (RDIs) [14] and standardized precipitation index (SPI) [15] to estimate the drought intensity of the region. (2) Evaluation of EEQ using comprehensive RS ecological indices built by coupling multiple indicators with certain models and computational methods, such as the pressure state response (PSR) model [16–19], ecological index (EI) [20], and a new RS ecological index (RSEI) which integrates four indexes (NDBSI, NDVI, WET, and LST) using principal component analysis (PCA) [21]. An increasing number of scholars have analyzed EEQ using RSEI in the study area [22–27], with further improvements and optimizations made based on RSEI [28–31].

However, individual ecological indicators used for evaluating the environment can only monitor specific types of environmental characteristics and cannot offer a holistic and comprehensive assessment of the complex eco-environment. Both the PSR model [16–19] and EI [20] necessitate numerous indicators, and difficulties remain in the collection of these indicators. Moreover, neither of these evaluation systems can directly illustrate the spatial features of EEQ within the research region. The RSEI, integrated using PCA, relies entirely on RS technology [21]. Its data requirements are easily obtainable, allowing for analyses over large areas, and the results are visualizable, addressing the limitations of the two previous methods. However, the contribution rate of RSEI derived from the normalization of the first component of the PCA (PC1) ranges from 60% to 90%, which does not guarantee a consistently high contribution rate [23–25]. In addition, due to the non-uniqueness of eigenvector directions in PCA [30], existing models may yield different results, sometimes misleading scholars to make wrong evaluations.

Based on coupling multiple RS ecological indicators and scientific evaluation of regional EEQ, it is important to explore more reasonable and effective coupling or calculation methods for deriving a comprehensive RS ecological index to support regional ecological protection. Copula function, as a tool for correlation analysis and multivariate modeling, has its unique advantages in dealing with nonlinear and asymmetric data. The Copula method and its application have attracted wide attention both domestically and internationally, and its scope of application has been expanding. In environmental sciences [32], it is suitable for multivariate hydrological analysis in hydrological research, such as extreme precipitation, flood frequency, drought characteristics analysis and drought prediction [33].

The Copula function has demonstrated high applicability and accuracy in constructing multivariate comprehensive drought indices, such as those involving temperature, precipitation, and runoff [34]. However, it has been less applied in the construction of multivariate comprehensive remote sensing ecological indices. The innovative approach of the research is inspired by the process of constructing multivariate comprehensive drought indices. Constructing a comprehensive RS ecological index of multiple indicators can be analogous to the problem of multivariable fitting analysis. The relationship between variables includes the correlation between each variable and their overall joint distribution relationship. The distribution function of an individual variable, that is, the marginal distribution function, describes the univariate information, while the joint distribution function describes the overall information. Therefore, in the research, a new comprehensive RS ecological index (CRSEI) based on the quaternion Copula function was innovatively constructed from remote sensing ecological indicators to comprehensively analyze spatiotemporal variation of eco-environment in the Henan Province of China. The main objectives of the research are: (1) to construct the CRSEI and conduct a comparative analysis of the autocorrelation between CRSEI, RSEI, and various ecological indicators, as well as the offsets between CRSEI, RSEI, and EI, to evaluate their applicability and accuracy in monitoring EEQ; (2) to examine the spatiotemporal evolution of EEQ in the Henan Province of China, based on CRSEI, including time-series changes, spatial distribution characteristics, and trend detection. The research provides a feasible approach for introducing the quaternion Copula function into the evaluation of EEQ.

2. Materials and Methods

2.1. Study Area

Henan Province (31°23′–36°22′N, 110°21′–116°39′E) primarily lies in the warm temperate zone, while its southern region borders the subtropical zone, belonging to the transition from the north subtropical zone to the warm temperate continental monsoon climate. Over the last decade, Henan Province has experienced average annual temperatures ranging from 12.9 °C to 16.5 °C, precipitation between 464.2 mm and 1193.2 mm, sunshine hours ranging from 1505.9 to 2230.7 h annually, and a frost-free period lasting between 208.7 and 290.2 days (www.henan.gov.cn) (accessed on 25 March 2023). The forest cover ranges from 12.52% to 20.16% (https://d.qianzhan.com/) (accessed on 25 March 2023). As shown in Figure 1, there are 5 regional divisions in Henan Province, including North Henan, South Henan, West Henan, East Henan, and Central Henan.

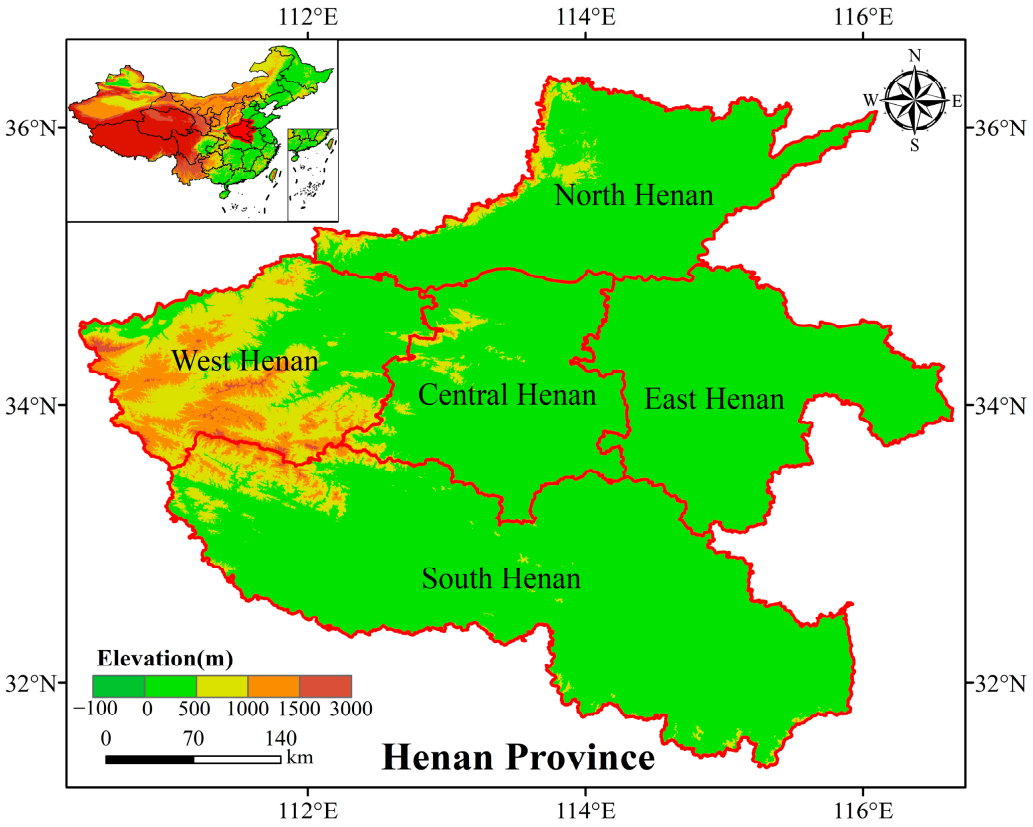

Figure 1. Study area.

2.2. Data

The ecological indicators of CRSEI and RSEI in the research were constructed based on MODIS data products from 2001–2020. The MODIS data products used in the research were obtained from two sources: (1) the Geospatial Data Cloud website from the Computer Network Information Center of the Chinese Academy of Sciences, and (2) the official website of the National Aeronautics and Space Administration (NASA). Since the China Geospatial Data Cloud website lacks MODIS data after 2016, 2001–2015 was selected as the time range to download the synthetic data products. The NDVI and LST for 2016 to 2020, along with other required data for 2001 to 2020, needed to be downloaded from NASA. The sources for research indicators and research data products are shown in Table 1.

Table 1. Research indicators and research data products.

Index	Data Product	Source	Time Span	Data Source
NDVI	MODND1M/ MOD11A1	GSCloud/ NASA	2001–2020	https://www.gscloud.cn/ https://www.earthdata.nasa.gov/ (accessed on 5 May 2023)
LST	MODLT1M/ MOD11A1	GSCloud/ NASA	2001–2020	https://www.gscloud.cn/ https://www.earthdata.nasa.gov/ (accessed on 5 May 2023)
WET	MOD09A1	NASA	2001–2020	https://www.earthdata.nasa.gov/ (accessed on 5 May 2023)
NDBSI	MOD09A1	NASA	2001–2020	https://www.earthdata.nasa.gov/ (accessed on 5 May 2023)
Ecological index (EI)	—	—	2001–2020	https://sthjt.henan.gov.cn/ (accessed on 10 July 2023)
—	monthly 1 km precipitation	TPDC	2001–2020	https://data.tpdc.ac.cn [35] (accessed on 15 October 2023)
—	1 km global land human footprint	—	2001–2020	https://www.x-mol.com/groups/li_xuecao/news/48145 [36] (accessed on 15 October 2023)
—	Digital elevation model (DEM)	NASA	—	https://search.asf.alaska.edu/ (accessed on 15 September 2024)
—	Land use types	RESDC	2001–2020	http://www.resdc.cn/ [37] (accessed on 15 September 2024)

Ecological index (EI) data were compiled in accordance with the *Technical Specifications for Ecological Environment Condition Evaluation (HJ 192-2015)* (https://www.mee.gov.cn/) (accessed on 15 September 2024), a national environmental protection standard of the People's Republic of China. EI is comprehensively represented by five sub-indices—the biological richness index, vegetation coverage index, water network denseness index, land stress index, and pollution load index—along with an environmental constraint index. These sub-indices reflect the richness of biological resources, the extent of vegetation cover, the availability of water resources, the intensity of land stress, and the pressure from pollution in the assessed region, respectively. The environmental constraint index serves as a restrictive indicator, adjusting the overall evaluation based on severe ecological damage or environmental pollution incidents that pose significant risks to human habitation and production safety [38]. It accurately reflects the region's ecological quality environment.

2.3. Methodology

Figure 2 shows the detailed workflow established by this research institute. MODIS data, with its global coverage, high spatial and temporal resolution, and short revisit period, facilitated the acquisition of comprehensive, high-resolution, monthly scale ecological indicators in this study. Four ecological indicators (NDVI, WET, NDBSI, LST) were derived through processing MODIS data products spanning from 2001 to 2020. RSEI and CRSEI were constructed using PCA and the quaternion Copula function, respectively. Subsequently, the applicability and monitoring accuracy of CRSEI were compared and analyzed.

Furthermore, spatiotemporal variation in the eco-environment quality (EEQ) of Henan Province from 2001 to 2020 was examined based on CRSEI data.

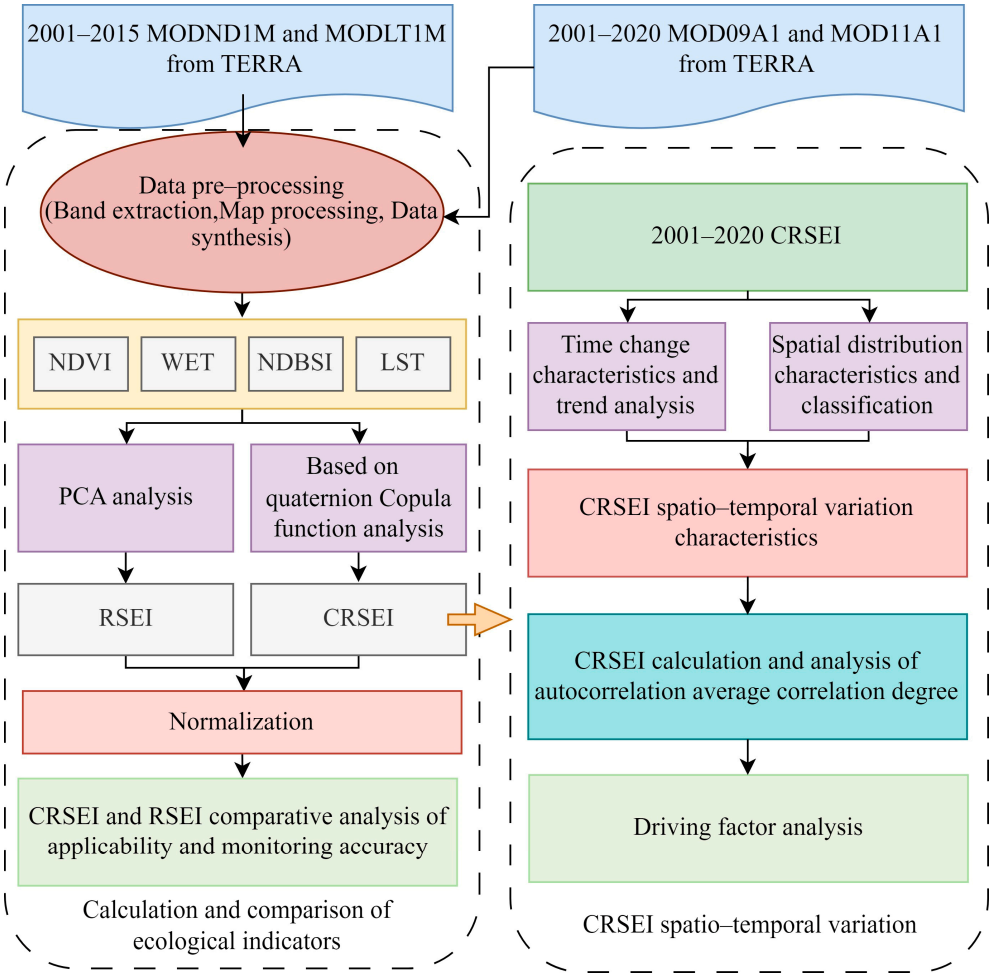

Figure 2. Flowchart of the research.

2.3.1. Remote Sensing Ecological Indicators

The ecological indicators utilized in the research encompass greenness (NDVI), humidity (WET), dryness (NDBSI), and heat (LST). The calculation and normalization methods for these four RS ecological indicators are as follows:

Greenness is expressed as *NDVI*, which is the most commonly used vegetation index to measure vegetation productivity due to its simplicity and robustness [39]. *NDVI* is expressed as:

$$NDVI = (NIR1 - Red)/(NIR1 + Red) \quad (1)$$

where *NIR*1, *Red*, are the reflectance of near infrared1, red light bands of MODIS images.

WET (humidity) can be calculated from remote sensing images by tasseled cap transformation algorithm [40]:

$$WETNESS = 0.1147B1 + 0.2408B2 + 0.3283B3 + 0.3132B4 - 0.3122B5 - 0.6416B6 - 0.5087B7 \quad (2)$$

where *B*1 to *B*7 represent bands 1–7 corresponding to the red, near infrared1(NIR1), blue, green, NIR2, short-wavelength infrared 1 (SWIR1), and SWIR2 bands of MODIS images, respectively.

This paper selected the index-based Build-up Index (*IBI*) [41] and Bare Soil Index (*BSI*) [42] to calculate the *NDBSI*. The formula is as follows:

$$\begin{gathered} BSI = [(SWIR1 + Red) - (NIR1 + Blue)]/[(SWIR1 + Red) + (NIR1 + Blue)] \\ IBI = \frac{\frac{2SWIR1}{SWIR1+NIR1} - \left(\frac{NIR1}{NIR1+Red} + \frac{Green}{Green+Blue}\right)}{\frac{2SWIR1}{SWIR1+NIR1} + \left(\frac{NIR1}{NIR1+Red} + \frac{Green}{Green+Blue}\right)} \\ NDBSI = (BSI + IBI)/2 \end{gathered} \tag{3}$$

where *SWIR*1, *NIR*1, *Red*, *Green*, and *Blue* are the reflectance of shortwave infrared1, near infrared1, red, green, and blue light bands of MODIS images, respectively.

Heat was represented by LST in the MODIS data product.

Monthly scale NDVI, WET, NDBSI, and LST were calculated for 240 months from 2001 to 2020 using the above formulas, respectively. Since the units of each ecological indicator would be different in the calculation process, the indicators were regularized and then subjected to PCA or Copula analysis. The regularization process can avoid the imbalance of weights on the results due to the different quantitative units, and it can reduce the differences in remote sensing images due to different seasons. The formulas for the formalization of each indicator are as follows:

$$NI_i = (I_i - I_{\min})/(I_{\max} - I_{\min}) \tag{4}$$

where NI_i is the value of a regularized indicator, I_i is the value of the indicator at image element, $I_{\max}$ is the maximum value of the indicator, and $I_{\min}$ is the minimum value of the indicator.

2.3.2. RSEI Index Construction

RSEI was obtained by coupling four indicators, *NDVI*, *WET*, *NDBSI* and *LST*, in the framework of the Pressure-State-Response (PSR) concept using principal component analysis (*PCA*) [21], with the first component of the PCA (*PC*1) denoting the RSEI. This was implemented so that images of the four normalized remote sensing eco-indicators mentioned above could be compared to the *RSEI* using the covariance matrix of *PC*1 and image analysis software using PCA functions (e.g., ARCGIS 10.8, ENVI 5.3.). The initial *RSEI*, $RSEI_0$, is then represented by *PC*1:

$$RSEI_0 = PC1[f(NDVI, WET, NDBSI, LST)] \tag{5}$$

The final *RSEI* was calculated according to the direction of the eigenvectors in the *PCA* analysis results. Since the direction of the eigenvectors of *NDVI* and *WET* calculated in this paper was positive, and the direction of the eigenvectors of *NDBSI* and *LST* calculated in this paper was negative, the *RSEI* was calculated using [30]:

$$RSEI = 1 - RSEI_0 = PC1[f(NDVI, WET, NDBSI, LST)] \tag{6}$$

2.3.3. CRSEI Index Construction Based on Quaternion Copula Function

In the research, four remote sensing ecological indexes (NDVI, WET, NDBSI, and LST) were coupled using the quaternion Copula function to construct CRSEI. The quaternion Copula function was used as the connecting tool of edge distribution function, and the quaternion Copula function parameters of NDVI, WET, NDBSI, and LST of each month were determined one pixel by one in parallel to complete the construction of joint distribution function. The function value was calculated by substituting the four index sequences into the quaternion Copula function after determining the parameters, and it was used as the CRSEI value of the pixel point.

The raster image data were processed in matrix form, and the monthly scale NDVI, WET, NDBSI, and LST time-series data, including 20 years and 240 months, were read one by one according to the pixels at the same location. That is, the first location pixel N_1 could read the four indicators as $NDVI_{N_1}(x_1, x_2, \ldots, x_{240}), WET_{N_1}(x_1, x_2, \ldots, x_{240})$,

$NDBSI_{N_1}(x_1, x_2, \ldots, x_{240})$, $LST_{N_1}(x_1, x_2, \ldots, x_{240})$ four time series, and read all the image points in turn. And through the Gringorten formula [43], each of the above indicators was calculated one by one like element points to construct the monthly scale time-series marginal distribution function of each indicator $U(X_1)$, $V(X_2)$, $G(X_3)$, $W(X_4)$. Each indicator's marginal distribution function contained a sequence of 240 terms. Subsequently, according to $\rho = sin(\frac{\pi\tau}{2})$, the τ of Kendall's correlation coefficient [44] was utilized to estimate the correlation coefficient matrix $\hat{\rho}$ of the four ecological indicators, and the great likelihood estimation method was applied to estimate the parameter of the degrees of freedom, $\hat{k}$. According to the Sklar's theorem, by comparing the joint distribution function of the four time series, namely NDVI, WET, NDBSI, and LST, the joint distribution function of the four time series can be deduced. Then, the following formula can be derived [45,46]:

$$P(x_1 \leq X_1, x_2 \leq X_2, x_3 \leq X_3, x_4 \leq X_4) = C[U(X_1), V(X_2), G(X_3), W(X_4)] = p \quad (7)$$

where x_1, x_2, x_3, x_4 are the four groups of time series of NDVI, WET, NDBSI, and LST correspond to variables; $U(X_1)$, $V(X_2)$, $G(X_3)$, $W(X_4)$ are the edge distribution functions of the four variables; p is the joint distribution function of the four variables. C is the corresponding Copula function.

$$\hat{\rho}_{ij} = \sin\left(\frac{\pi\hat{\tau}_{ij}}{2}\right),\ i = 1, 2, 3, 4;\ j = 1, 2, 3, 4 \quad (8)$$

$$\hat{k} = \arg\max_{k\in(2,\infty]} \log(c(u_1, u_2, u_3, u_4; \rho, k)) \quad (9)$$

The expressions for the distribution function and density function of the quaternion Copula function [47]:

$$\begin{aligned} C(u_1, u_2, u_3, u_4; \rho, k) &= t_{\rho,k}\left[t_k^{-1}(u_1), t_k^{-1}(u_2), t_k^{-1}(u_3), t_k^{-1}(u_4)\right] \\ c(u_1, u_2, u_3, u_4; \rho, k) &= |\rho|^{-\frac{1}{2}} \frac{\Gamma\left(\frac{k+4}{2}\right)\left[\Gamma\left(\frac{k}{2}\right)\right]^4\left(1 + \frac{1}{k}\zeta^{-1}\rho^{-1}\zeta\right)^{-\frac{k+4}{2}}}{\left[\Gamma\left(\frac{k+1}{2}\right)\right]^4\Gamma\left(\frac{k}{2}\right)\prod_{i=1}^{4}\left(1 + \frac{\zeta_i^2}{k}\right)^{-\frac{k+1}{2}}} \end{aligned} \quad (10)$$

where C is the distribution function of the quaternion Copula function; c is density function of the quaternion Copula function; ρ is a symmetric positive definite matrix of order 4 with all elements of 1 on the diagonal; $|\rho|$ denotes the determinant of the square matrix ρ; u_1, u_2, u_3, u_4 correspond to the marginal distribution function above $U(X_1)$, $V(X_2)$, $G(X_3)$, $W(X_4)$; $t_{\rho,k}$ denotes the distribution function of the standard quaternion t distribution with correlation coefficient matrix of ρ and degrees of freedom of k; t_k^{-1} denotes the inverse function of the standard cell distribution function t distribution with degree of freedom k, ζ, as follows:

$$\zeta = \left[t_k^{-1}(u_1), t_k^{-1}(u_2), t_k^{-1}(u_3), t_k^{-1}(u_4)\right] \quad (11)$$

The CRSEI value was calculated according to the location of each image point and time information to regenerate the visualization of raster data, and it was normalized, making it easy to compare and analyze with RSEI. To better analyze the EEQ features in Henan Province, the CRSEI value located in [0, 1] was divided into five levels in Table 2.

Table 2. CRSEI levels.

LV.	CRSEI Levels	CRSEI Value
1	Poor	$0 \leq$ Index < 0.2
2	Fair	$0.2 \leq$ Index < 0.4
3	Moderate	$0.4 \leq$ Index < 0.6
4	Good	$0.6 \leq$ Index < 0.8
5	Excellent	$0.8 \leq$ Index

2.3.4. Average Correlation Analysis and Sen's Slope and Modified Mann-Kendall (Sen + MMK) Trend Analysis

The average correlation is expressed as the average of the absolute values of the correlation coefficients of an indicator and others in the same period, with the following formula:

$$\overline{C_P} = \frac{|C_S + C_Q + \ldots + C_R|}{n} \quad (12)$$

where $\overline{C_P}$ is the average correlation of indicator P; C_S, C_Q, …, C_R denote the correlation coefficients of the same-period indicators: S, Q, …, R, respectively; n is the number of same-period indicators.

The Theil–Sen Median method, also known as Sen's slope estimation, is a method for computing nonparametric statistical series data. The method is extremely computationally efficient for analysis of trends in long-term time-series data, but is not sensitive to the reflection of computational and measurement errors in outlier data [48].

$$S = mean\left(\frac{X_j - X_i}{j - i}\right), \forall j > i \quad (13)$$

where X_j and X_i are time-series data. $S > 0$ indicates an upward trend in the time series; $S < 0$ indicates a downward trend in the time series.

The modified Mann–Kendall trend test method (MMK) [49], which has significantly improved the test ability to directly reflect the effect of MK method, has been greatly applied to the current flood and drought meteorology and other fields.

3. Results

3.1. Comparative Analysis of RSEI and CRSEI

3.1.1. Comparative Analysis of Applicability

The correlation coefficients between each ecological indicator and the monthly and annual CRSEI and RSEI scales are statistically presented in Figure 3. The correlation coefficients of CRSEI with the ecological indicators were slightly higher than those of RSEI, indicating a strong correlation between CRSEI and RSEI, thus making CRSEI suitable for eco-environment quality (EEQ) research. Furthermore, both CRSEI and RSEI exhibited positive correlations with WET and NDVI and negative correlations with NDBSI and LST. The correlation coefficients of CRSEI with NDVI, WET, NDBSI, and LST were 0.8724, 0.6477, −0.7422, and −0.6934 on the annual scale and 0.9274, 0.8033, −0.7629, and −0.8755 on the monthly scale. The correlation coefficients for RSEI were 0.7672, 0.5124, −0.7077, and −0.5148 on the annual scale and 0.8416, 0.7505, −0.7282, and −0.5876 on the monthly scale.

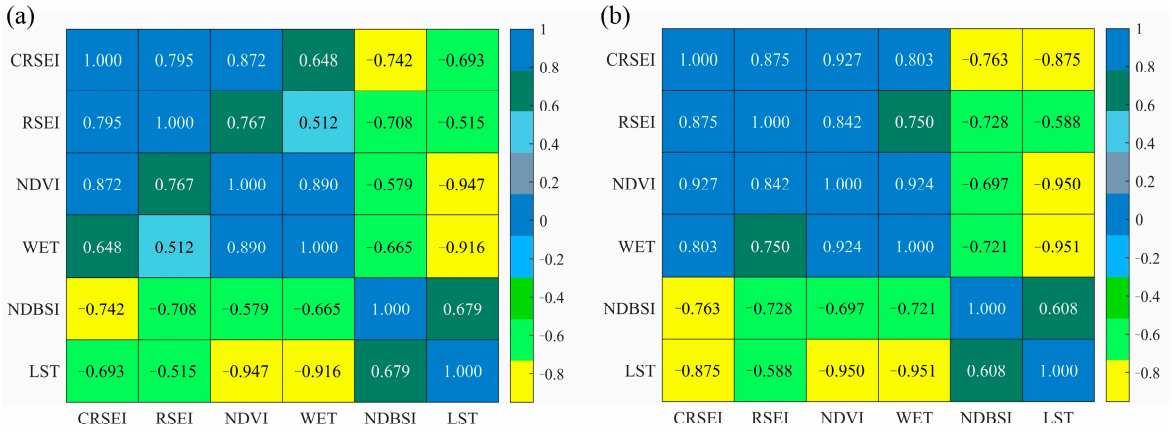

Figure 3. Matrix of correlation coefficients between CRSEI, RSEI and each ecological indicator (NDVI, WET, NDBSI, LST). (**a**) Annual scale; (**b**) monthly scale.

In Figure 4, the average correlation between CRSEI and RSEI exceeded 0.8 in all 20 years from 2001 to 2020. Notably, their average correlation was greater than 0.9 in the years 2001, 2011, and 2020. Specifically, in 17 out of the 20 years, the average correlation of the CRSEI exceeded that of the RSEI, with the exception of 2013, 2015, and 2016, when the average correlation of the CRSEI fell slightly below that of the RSEI. The average correlation of CRSEI was lower than that of RSEI by 0.015, 0.051, and 0.009, respectively.

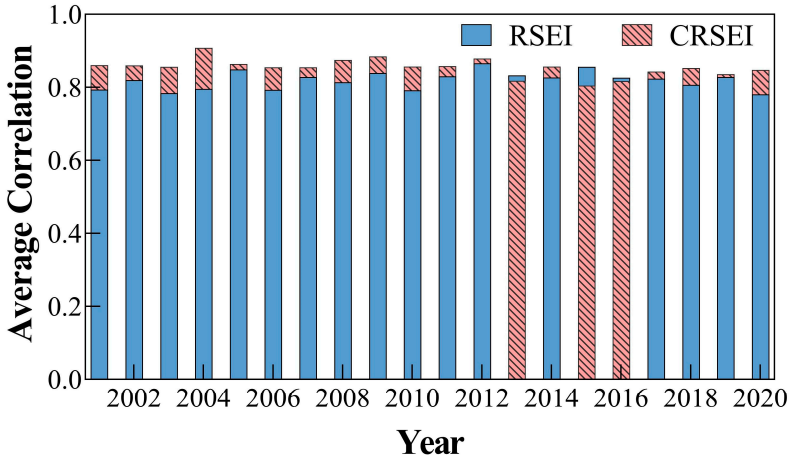

Figure 4. Stack map of ecological index RSEI and CRSEI average correlation.

3.1.2. Comparative Analysis of Monitoring Accuracy

Figure 5 illustrates the eco-environment quality level changes and relative EI offsets of CRSEI and RSEI in Henan Province from 2001 to 2020. Although the EI and CRSEI were coupled with different ecological indicators and used different methods, the normalization results of CRSEI were closer to the official announcement EI than those of RSEI. Numerically, the offsets of CRSEI were smaller than those of RSEI in most years. The maximum and minimum offsets for RSEI versus EI were 0.1753 and 0.0112, respectively, while for CRSEI versus EI, they were 0.0991 and 0.0016, respectively. These values were much smaller than those of RSEI. CRSEI had an average offset 123% lower than that of RSEI. Hence, the overall monitoring results of the CRSEI, constructed based on the quaternion Copula function, are more accurate.

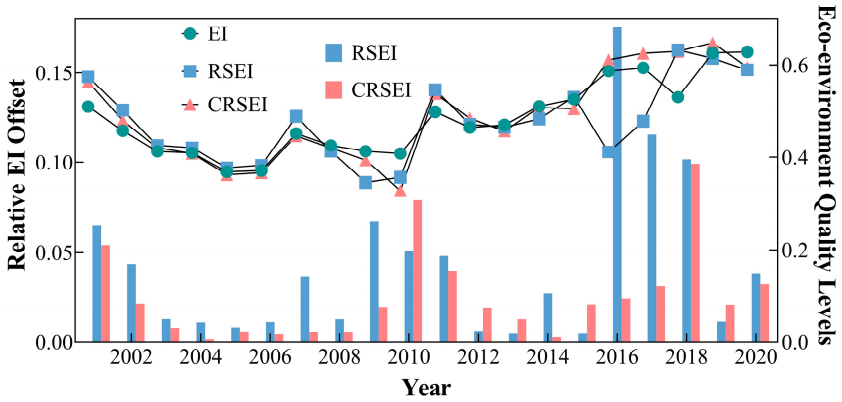

Figure 5. Eco-environment quality levels change and relative EI offsets of CRSEI and RSEI from 2001 to 2020 in Henan Province.

3.2. Temporal and Spatial Variations of CRSEI

3.2.1. Temporal Variation

Figure 6 illustrates the distribution of CRSEI data in Henan Province from 2001 to 2020. The median of CRSEI statistics exhibited a downward trend followed by an upward

trend, with the lowest median value occurring in 2010. Additionally, most of the quartiles before 2010 were smaller than those after 2010.The results indicate that the EEQ of Henan Province declined from 2001 to 2010 but improved significantly and rebounded from 2011 to 2022.The year 2010 marked the lowest EEQ during the observed period.

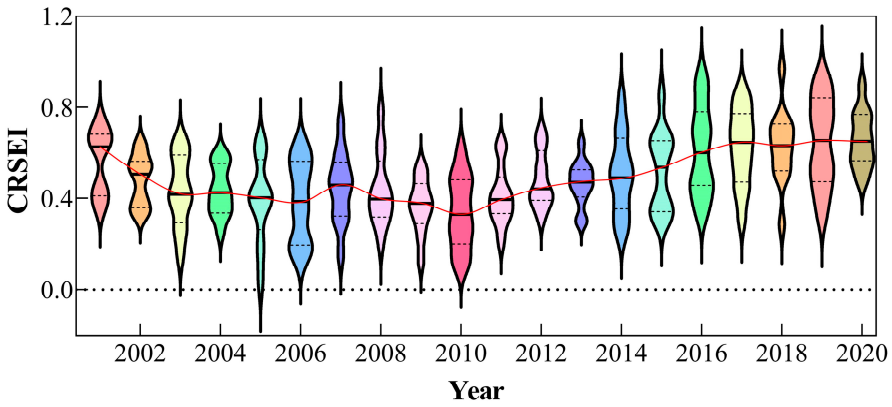

Figure 6. Distribution of CRSEI data from 2001 to 2020 in Henan Province.

Figure 7 depicts the changes in CRSEI for each geographical division of Henan Province from 2001 to 2020. Overall, there was an initial downward trend followed by an upward trend in CRSEI values for all regions. Additionally, West Henan exhibited higher CRSEI values compared to the other regions. The minimum value for each region was observed in 2010, with respective values of 0.4890, 0.5013, 0.4930, 0.4932, and 0.4912, with West Henan recording the highest value and Central Henan the lowest. The maximum value for each region occurred in 2020, indicating a significant improvement in EEQ. The respective values, in the same order as mentioned above, were 0.6654, 0.7753, 0.6759, 0.6289, and 0.6015. Notably, West Henan and South Henan recorded the highest values, while Central Henan recorded the lowest.

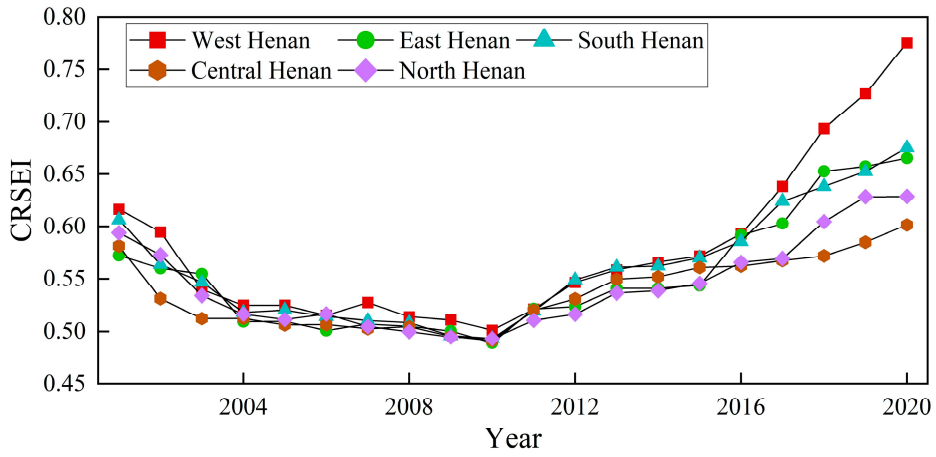

Figure 7. CRSEI variation from 2001 to 2020 in various regional subdivisions of Henan Province.

Figure 8 shows the seasonal variation of CRSEI in each geographical division of Henan Province from 2001 to 2020. Overall, the CRSEI values for each season in West Henan were higher than those in other regions. The seasonal CRSEI values across different regions exhibited a trend similar to that of the annual values, initially decreasing and then subsequently increasing. The CRSEI values in spring and summer were higher than those in autumn and winter, indicating that the EEQ in Henan Province is superior in spring and summer compared to autumn and winter. The maximum seasonal CRSEI values in each region were observed in the spring or summer of 2020, indicative of significant restoration in the EEQ of Henan Province since 2010.

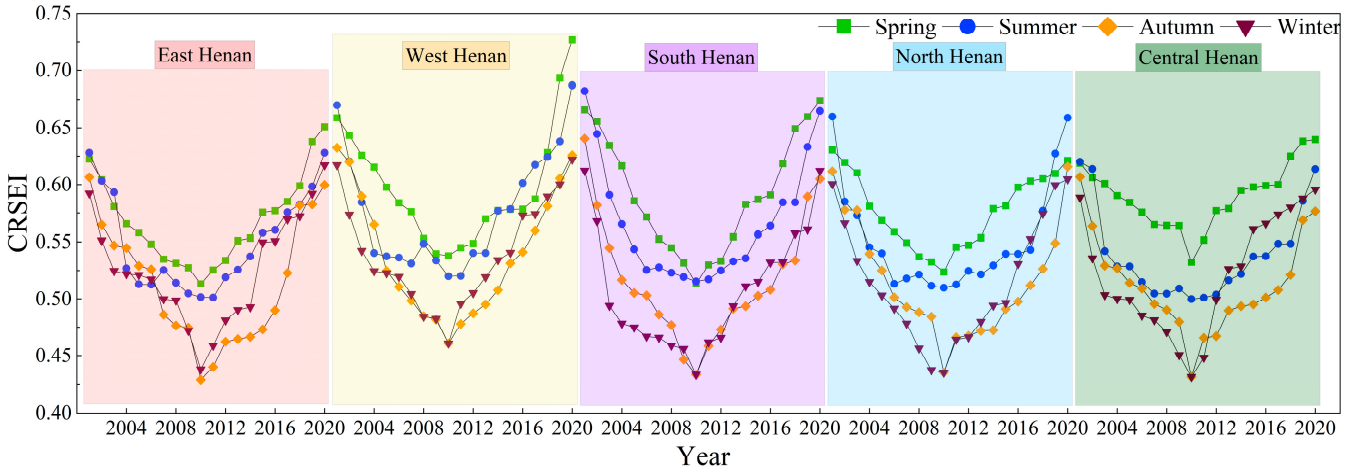

Figure 8. Seasonal CRSEI variation from 2001 to 2020 in various regional subdivisions of Henan Province.

3.2.2. Spatial Variation

Figure 9 shows the spatial distribution of CRSEI eco-environment quality levels from 2001 to 2020 in Henan Province. The EEQ levels of Henan Province were primarily poor and medium from 2001 to 2010 and medium and good after 2010. From 2001 to 2020, the EEQ levels of the West and South Henan Province were high, and they were all in the middle or above; the EEQ levels of the Central and East Henan Province were low, and the EEQ levels were basically below medium. Overall, from 2001 to 2010, the EEQ levels across most regions in Henan Province exhibited a significant downward trend, predominantly characterized by fair and poor levels. Notably, in 2010, the ecological levels reached their nadir, with the majority of Henan Province manifesting poor EEQ. From 2011 to 2020, the EEQ levels in Henan Province predominantly fell within the medium and above range. By 2020, most areas in Henan exhibited excellent EEQ levels, indicating a significant improvement in EEQ.

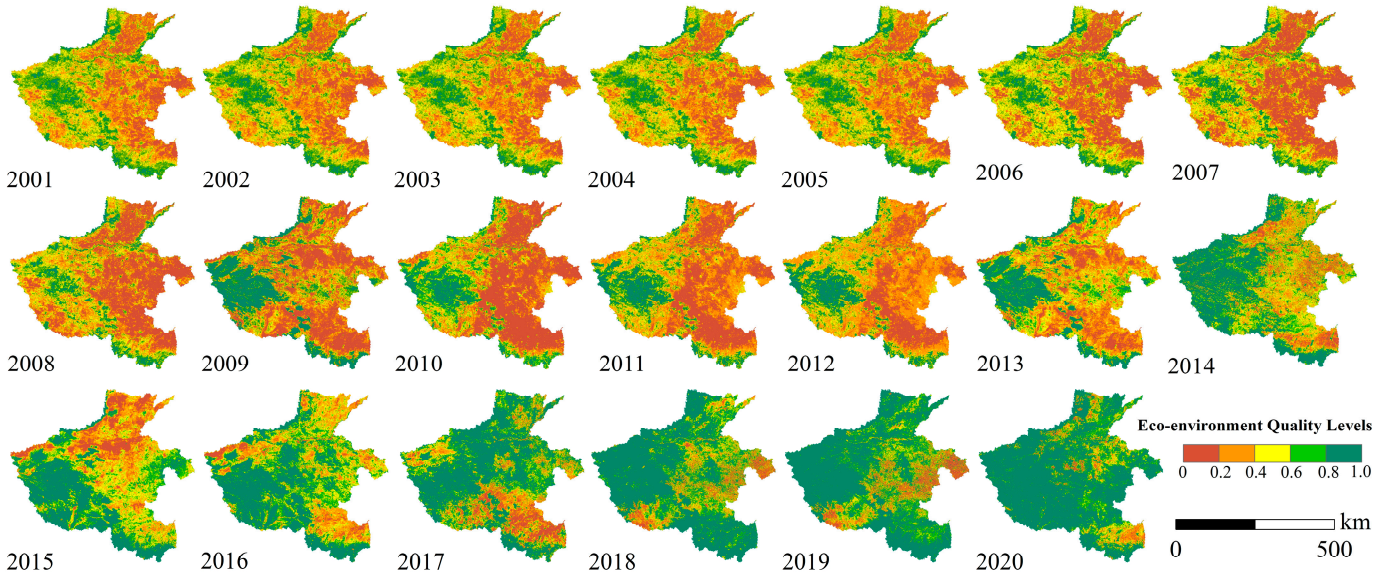

Figure 9. The spatial distribution of CRSEI eco-environment quality levels from 2001 to 2020 in Henan Province.

Figure 10 presents statistics on the variation in the proportion of each level of EEQ from 2001 to 2020 in Henan Province. The proportion of EEQ levels "poor" and "fair" exhibited

an increasing trend from 2001 to 2010, with "poor" reaching its peak at 68.3% in 2010, whereas "excellent" accounted for merely 2%. In addition, the percentages of "moderate" and "good" levels declined during this period. From 2011 to 2020, the percentages of "good" and "excellent" EEQ levels significantly rebounded, with a noticeable decline in the percentages of "poor", "fair" and "moderate". In 2020, the proportion of EEQ level "excellent" reached 74%, while the proportion of EEQ level "poor" was reduced to only 2%. These trends indicated a marked improvement in the EEQ of Henan Province over the past two decades.

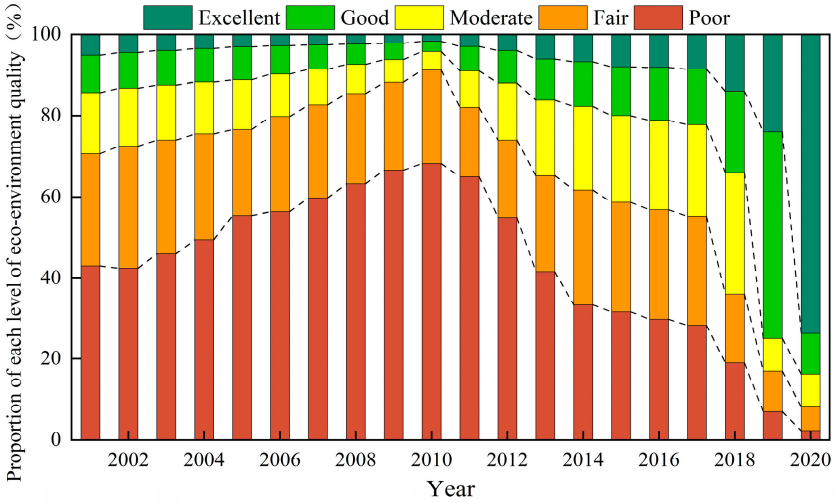

Figure 10. The variation in the proportion of each level of eco-environment quality from 2001 to 2020 in Henan Province.

Based on the raster seasonal and annual scale time series of CRSEI in Henan Province from 2001 to 2020, raster images depicting statistics Slope and Zs were generated using Sen + MMK trend analysis to determine spatial trends, as illustrated in Figures 11 and 12. For the period from 2001 to 2020, in most areas of Henan Province, where Slope > 0 and $1.65 < Zs < 1.96$, there was an indication of a slightly significant improvement trend in EEQ. Where Slope > 0 and $Zs > 1.96$, a significant improvement trend in EEQ was indicated, predominantly in the central region of Henan Province. In a few areas, where Slope < 0 and $-1.65 < Zs < -1.96$, a slight deterioration trend in EEQ was indicated, primarily in the southern region of Henan Province. Seasonally, the overall performance aligned more closely with annual trend changes, with EEQ improvement in Henan Province being more pronounced during spring and summer compared to fall and winter. In the central region of Henan Province, the trend toward EEQ improvement surpassed that in other regions across all four seasons.

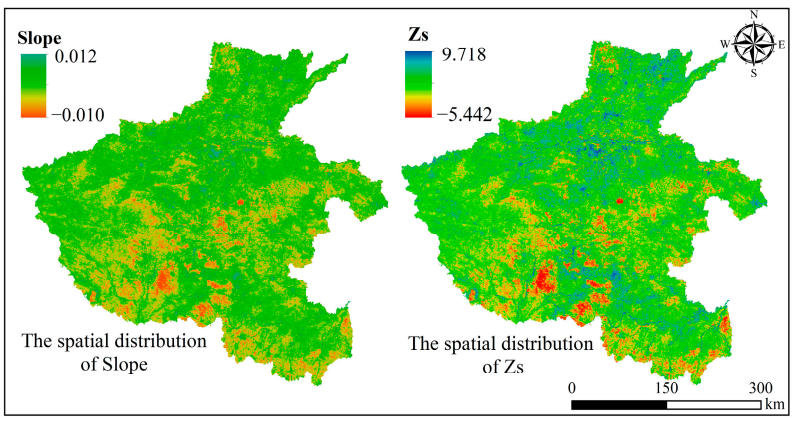

Figure 11. Results of Sen + MMK trend analysis of CRSEI at the annual scale in Henan Province.

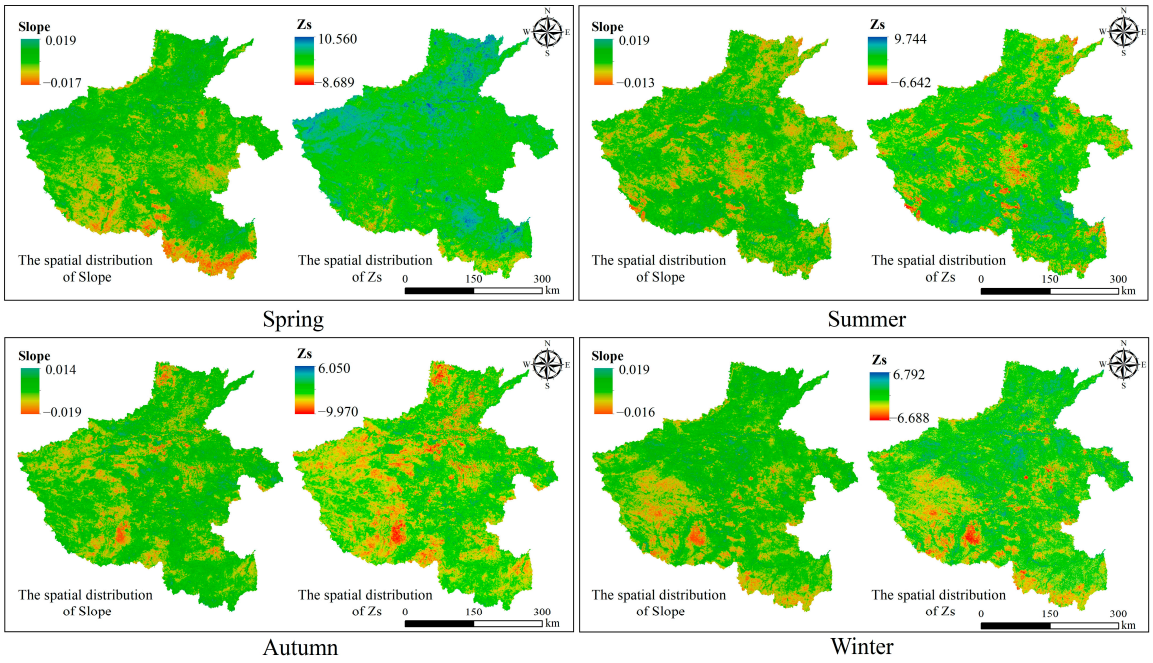

Figure 12. Results of Sen + MMK trend analysis of CRSEI at the seasonal scale in Henan Province.

4. Discussion

4.1. CRSEI Drivers Analysis

The research conducted random point sampling of CRSEI, human footprints, and precipitation in the study area and used Pearson correlation coefficient to analyze the correlation between intensity of human footprints and precipitation and CRSEI to infer the potential reasons for CRSEI changes.

In Figure 13, the correlation coefficients between eco-environment quality (EEQ) and human footprints predominantly ranged from −0.6 to −0.5 over the past two decades, indicating a strong negative correlation between EEQ and human footprints, with the maximum absolute value reaching 0.6414. These results align with other scholars' studies, which indicate that human-induced destruction and climatic conditions are the main causes of ecosystem degradation [50,51]. Precipitation, as a climatic factor directly affecting EEQ, had correlation coefficients with EEQ mostly in the range from 0.3 to 0.4, indicating a positive correlation, with the maximum value recorded at 0.4321. This is consistent with Zhang's (2022) research that precipitation and RSEI remained between 0.22 and 0.53 [52]. Furthermore, the correlation between human footprints and EEQ significantly exceeded that of precipitation, underscoring the substantial influence of human activities on EEQ.

Figure 14 illustrates a strong correlation between EEQ and human factors in most areas of Henan Province. The central and eastern areas of Henan exhibited an extremely strong correlation. EEQ and precipitation were correlated across nearly the entire Henan Province. This result aligns with the view of other scholars that the EEQ is influenced by both natural conditions and human factors [52,53].

The research further utilized the extraction of elevation from digital elevation model (DEM) data to analyze its correlation with CRSEI and compared CRSEI across different land use types.

Figure 15 illustrates the correlation between elevation and CRSEI, with a correlation coefficient of $r > 0.8$, indicating a strong relationship. This suggests that EEQ in Henan Province improves with increasing elevation. Figure 16 presents the distribution of CRSEI across different land use types, showing that forests have the highest CRSEI, followed by grassland, while urban exhibit the lowest CRSEI. This demonstrates that urban expansion negatively impacts EEQ [54].

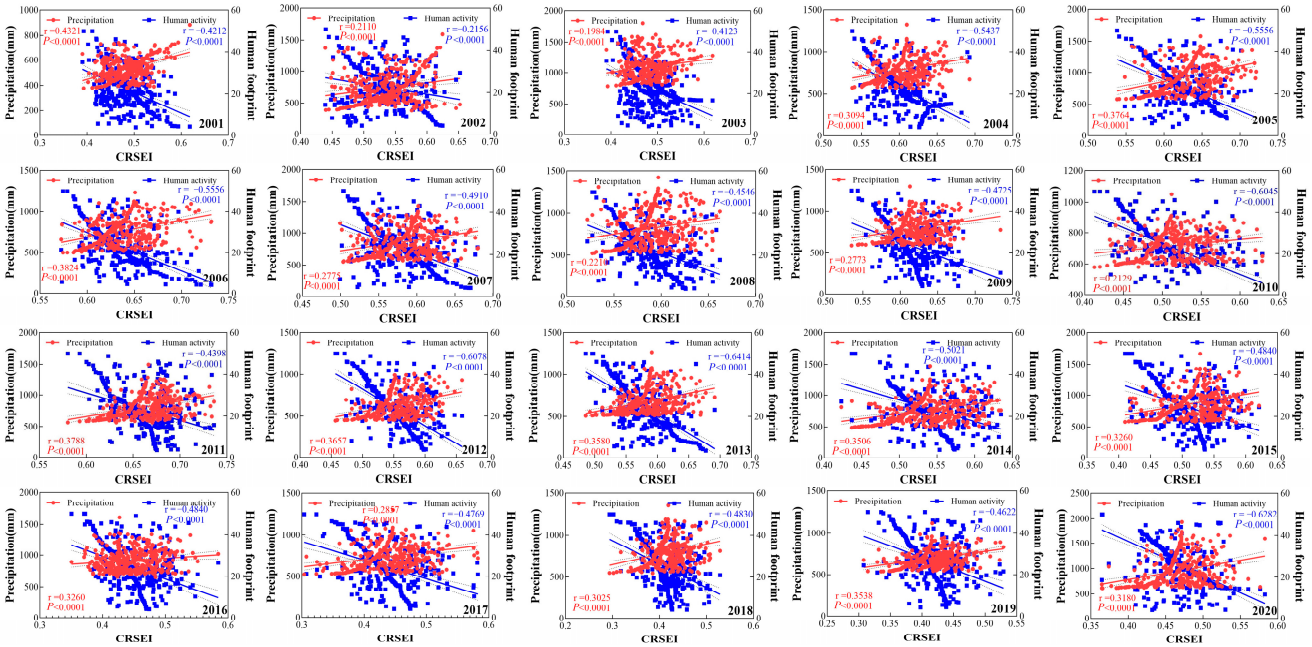

Figure 13. Correlation of CRSEI with human footprint and precipitation.

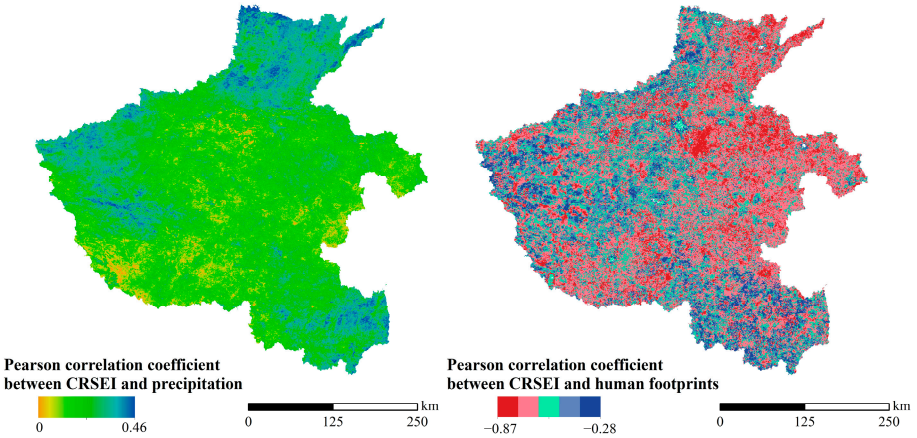

Figure 14. Spatial distribution of CRSEI with human footprint and precipitation correlation coefficients.

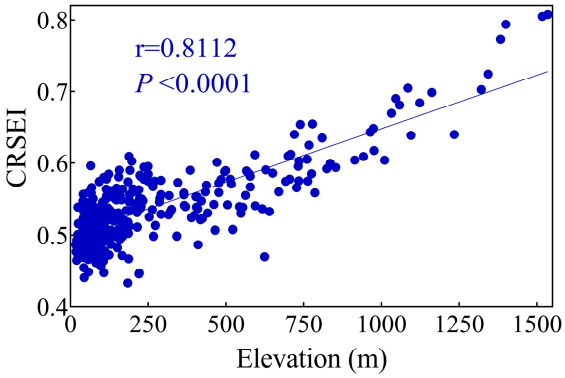

Figure 15. Correlation of CRSEI with elevation.

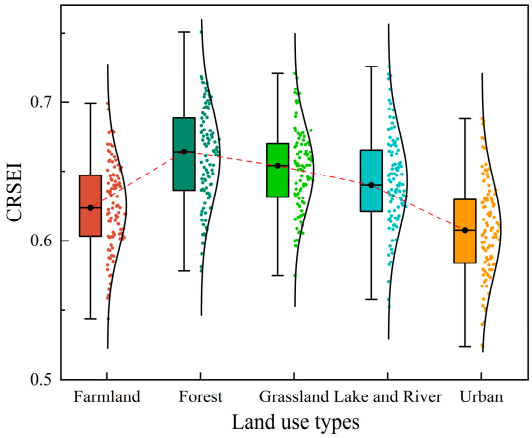

Figure 16. Distribution of CRSEI in different land use types in Henan Province.

The rapid urban expansion propelled by Henan Province's economic development from 2001 to 2010, followed by a slowdown in urban growth from 2010 to 2020 [55], along with the ecological restoration promoted by China's ecological restoration program [56,57], resulted in a sustained decline in EEQ from 2001 to 2010 and a steady recovery from 2010 to 2020. Henan Province is situated in north-central China, with a climate marked by rainy summers and dry winters. Since EEQ was positively correlated with precipitation, the ecological quality was higher in spring and summer and lower in fall and winter. Three consecutive years of below-average precipitation from 2008 to 2010 also contributed to the lowest EEQ in 2010. West and South Henan are predominantly mountainous and hilly, with extensive forests and grasslands, dense vegetation cover, and little human activity. As a result, the EEQ in West and South Henan was significantly better compared to other areas. North Henan, primarily grassland with relatively minimal human activities, also enjoyed better ecological quality. In contrast, Central Henan, which includes the capital city, is densely populated, with little vegetation and intensive human activities, leading to poorer ecological quality. East Henan, situated in the plains, consists mainly of farmland with sparse vegetation cover, resulting in moderate EEQ.

4.2. Strengths, Limitations, and Future Prospects

The novelty of the research is that the quaternion Copula function was introduced into the calculation of the integrated ecological index of remote sensing. The quaternion Copula function was used to combine four ecological indicators to construct a new remote sensing index (CRSEI). This is different from the previous RSEI based on PCA [21] and TDG calculated by the three-dimensional greenness model, which replaces the NDVI of RSEI to build TDRSEI [28]. In Figure 17, the R^2 and Pearson correlation coefficients of CRSEI with EI were higher than those of RSEI. Furthermore, the R^2 value of 0.8778 for CRSEI with EI further underscores the accuracy of CRSEI. CRSEI was employed to evaluate the EEQ in Henan Province, demonstrating greater applicability and monitoring accuracy than RSEI.

The current research is subject to limitations due to restricted research capacity and data collection. Firstly, the calculation process of the quaternion Copula function is complex, and the vast amount of data regarding raster RS ecological indicators based on time series demands substantial computing power. Secondly, the ecological indicators used in the research were derived solely from those studied in RSEI, with no additional indices included. However, EEQ is usually affected by multiple factors.

According to the characteristics of the Copula function, we can freely choose the number of ecological indicators to calculate CRSEI. We plan to introduce new ecological indicators, such as air quality and soil water content, to provide a more comprehensive assessment of EEQ. In the future, we will design a concise and efficient parallel computing program to accelerate the calculation of the multivariate Copula function based on raster

image sequences. We will introduce additional ecological indicators to construct the CRSEI for a comprehensive assessment of the EEQ in larger study areas.

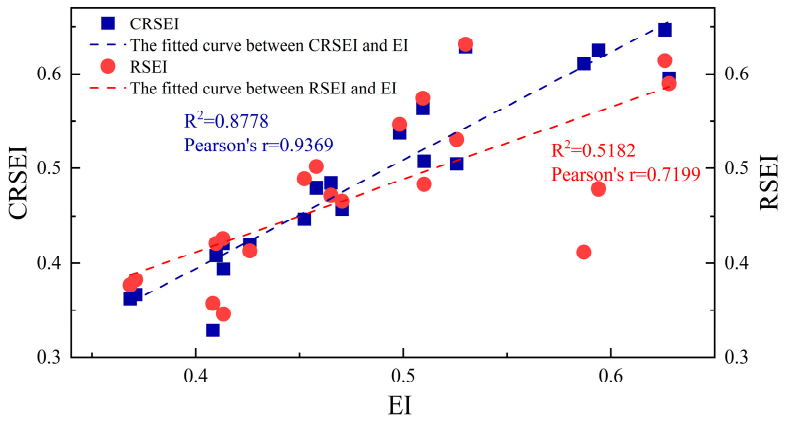

Figure 17. R^2 and correlation coefficient of EI with CRSEI and RSEI.

5. Conclusions

The research constructs a new comprehensive RS ecological index (CRSEI) based on the quaternion Copula function and compares and analyzes its applicability and detection accuracy with RSEI. The research utilized CRSEI to monitor and evaluate the spatiotemporal dynamics of the eco-environment quality (EEQ) in Henan Province over the past two decades. The main conclusions of the research are as follows.

(1) The average correlation coefficients of CRSEI and RSEI in Henan Province in the past 20 years both exceeded 0.8, indicating a strong correlation, and the average correlation of CRSEI in the past 17 years was higher than that of RSEI. The average correlation test of CRSEI outperformed that of RSEI. The maximum and minimum offsets of CRSEI relative to EI were smaller than those of RSEI. The average offset of RSEI was 123% higher than that of CRSEI. Therefore, CRSEI is more scientific and accurate than RSEI, making it suitable for EEQ assessment.

(2) The EEQ of Henan Province declined from 2001 to 2010 and improved and rebounded significantly from 2011 to 2020, with the lowest median value in 2010. In all regions, the CRSEI value was larger in West and South Henan and the smallest in Central Henan. In addition, CRSEI value in West Henan was higher than in other areas during all seasons. The minimum value of CRSEI in Central Henan in 2010 was 0.4912, and the maximum value was 0.7753 in West Henan in 2010.

(3) The EEQ in Henan Province showed deterioration from the central cities to the periphery and then improvement from the periphery to the center. From 2001 to 2010, the EEQ continued to deteriorate. In 2010, regions with poor EEQ level made up 68.3% of the total area, while only 2% were rated as excellent; From 2011 to 2020, Henan Province EEQ improved and became better, and by 2020, regions with excellent EEQ level constituted 74% of the total area.

The research provided a feasible approach to introduce the quaternion Copula function into the evaluation of EEQ and demonstrated the high applicability and accuracy of CRSEI. Future studies plan to introduce other ecological indicators to construct the CRSEI to provide a more accurate and comprehensive assessment of environmental quality in larger study areas.

Author Contributions: Conceptualization, Z.W. and H.Y.; methodology, H.Y., L.H. and Q.L.; validation, Z.D.; formal analysis, L.H.; writing—original draft preparation, L.H.; writing—review and editing, Z.W., H.Y., Y.Z. and F.C.; funding acquisition, H.Y. All authors have read and agreed to the published version of the manuscript.

Funding: This research was funded by the National Key R&D Program of China(2021YFC3200205), the Henan provincial key research and development program (221111321100), the Excellent Youth Foundation of He'nan Scientific Committee (222300420013), the Significant Science and Technology Project of Ministry of Water Resources (SKS-2022011).

Data Availability Statement: Data are contained within the article.

Acknowledgments: We are grateful to the editors and anonymous reviewers for their thoughtful comments.

Conflicts of Interest: The authors declare no conflicts of interest.

References

1. McDonnell, M.J.; MacGregor-Fors, I. The ecological future of cities. *Science* **2016**, *352*, 936–938. [CrossRef] [PubMed]
2. Levin, S.A. The Problem of Pattern and Scale in Ecology: The Robert H. MacArthur Award Lecture. *Ecology* **1992**, *73*, 1943–1967. [CrossRef]
3. Ji, J.; Tang, Z.; Zhang, W.; Liu, W.; Jin, B.; Xi, X.; Wang, F.; Zhang, R.; Guo, B.; Xu, Z.; et al. Spatiotemporal and Multiscale Analysis of the Coupling Coordination Degree between Economic Development Equality and Eco-Environmental Quality in China from 2001 to 2020. *Remote Sens.* **2022**, *14*, 737. [CrossRef]
4. Pettorelli, N.; Vik, J.O.; Mysterud, A.; Gaillard, J.-M.; Tucker, C.J.; Stenseth, N.C. Using the satellite-derived NDVI to assess ecological responses to environmental change. *Trends Ecol. Evol.* **2005**, *20*, 503–510. [CrossRef]
5. Li, Y.; Cao, Z.; Long, H.; Liu, Y.; Li, W. Dynamic analysis of ecological environment combined with land cover and NDVI changes and implications for sustainable urban–rural development: The case of Mu Us Sandy Land, China. *J. Clean. Prod.* **2017**, *142*, 697–715. [CrossRef]
6. Ramírez-Cuesta, J.M.; Minacapilli, M.; Motisi, A.; Consoli, S.; Intrigliolo, D.S.; Vanella, D. Characterization of the main land processes occurring in Europe (2000–2018) through a MODIS NDVI seasonal parameter-based procedure. *Sci. Total Environ.* **2021**, *799*, 149346. [CrossRef]
7. Fattori Junior, I.M.; dos Santos Vianna, M.; Marin, F.R. Assimilating leaf area index data into a sugarcane process-based crop model for improving yield estimation. *Eur. J. Agron.* **2022**, *136*, 126501. [CrossRef]
8. Eliades, M.; Bruggeman, A.; Djuma, H.; Christofi, C.; Kuells, C. Quantifying Evapotranspiration and Drainage Losses in a Semi-Arid Nectarine (*Prunus persica* var. *nucipersica*) Field with a Dynamic Crop Coefficient (Kc) Derived from Leaf Area Index Measurements. *Water* **2022**, *14*, 734. [CrossRef]
9. Kyparissis, A.; Levizou, E. Climatic Drivers of the Complex Phenology of the Mediterranean Semi-Deciduous Shrub *Phlomis fruticosa* Based on Satellite-Derived EVI. *Plants* **2022**, *11*, 584. [CrossRef]
10. Buyantuyev, A.; Wu, J. Urban heat islands and landscape heterogeneity: Linking spatiotemporal variations in surface temperatures to land-cover and socioeconomic patterns. *Landsc. Ecol.* **2010**, *25*, 17–33. [CrossRef]
11. Singh, P.; Kikon, N.; Verma, P. Impact of land use change and urbanization on urban heat island in Lucknow city, Central India. A remote sensing based estimate. *Sustain. Cities Soc.* **2017**, *32*, 100–114. [CrossRef]
12. Mandal, J.; Patel, P.P.; Samanta, S. Examining the expansion of Urban Heat Island effect in the Kolkata Metropolitan Area and its vicinity using multi-temporal MODIS satellite data. *Adv. Space Res.* **2022**, *69*, 1960–1977. [CrossRef]
13. Xiong, L.; Li, S.; Zou, B.; Peng, F.; Fang, X.; Xue, Y. Long Time-Series Urban Heat Island Monitoring and Driving Factors Analysis Using Remote Sensing and Geodetector. *Front. Environ. Sci.* **2022**, *9*, 828230. [CrossRef]
14. Moghimi, M.M.; Zarei, A.R.; Mahmoudi, M.R. Seasonal drought forecasting in arid regions, using different time series models and RDI index. *J. Water Clim. Chang.* **2020**, *11*, 633–654. [CrossRef]
15. Banimahd, S.A.; Khalili, D. Factors Influencing Markov Chains Predictability Characteristics, Utilizing SPI, RDI, EDI and SPEI Drought Indices in Different Climatic Zones. *Water Resour. Manag.* **2013**, *27*, 3911–3928. [CrossRef]
16. Boori, M.S.; Choudhary, K.; Paringer, R.; Kupriyanov, A. Eco-environmental quality assessment based on pressure-state-response framework by remote sensing and GIS. *Remote Sens. Appl. Soc. Environ.* **2021**, *23*, 100530. [CrossRef]
17. Xiong, J.; Li, W.; Zhang, H.; Cheng, W.; Ye, C.; Zhao, Y. Selected Environmental Assessment Model and Spatial Analysis Method to Explain Correlations in Environmental and Socio-Economic Data with Possible Application for Explaining the State of the Ecosystem. *Sustainability* **2019**, *11*, 4781. [CrossRef]
18. Das, S.; Pradhan, B.; Shit, P.K.; Alamri, A.M. Assessment of Wetland Ecosystem Health Using the Pressure–State–Response (PSR) Model: A Case Study of Mursidabad District of West Bengal (India). *Sustainability* **2020**, *12*, 5932. [CrossRef]
19. Bai, X.; Tang, J. Ecological Security Assessment of Tianjin by PSR Model. *Procedia Environ. Sci.* **2010**, *2*, 881–887. [CrossRef]
20. Sun, R.; Wu, Z.; Chen, B.; Yang, C.; Qi, D.; Lan, G.; Fraedrich, K. Effects of land-use change on eco-environmental quality in Hainan Island, China. *Ecol. Indic.* **2020**, *109*, 105777. [CrossRef]
21. Xu, H. A remote sensing index for assessment of regional ecological changes. *China Environ. Sci.* **2013**, *33*, 889–897.
22. Xu, H.; Wang, Y.; Guan, H.; Shi, T.; Hu, X. Detecting Ecological Changes with a Remote Sensing Based Ecological Index (RSEI) Produced Time Series and Change Vector Analysis. *Remote Sens.* **2019**, *11*, 2345. [CrossRef]

23. Yuan, B.; Fu, L.; Zou, Y.; Zhang, S.; Chen, X.; Li, F.; Deng, Z.; Xie, Y. Spatiotemporal change detection of ecological quality and the associated affecting factors in Dongting Lake Basin, based on RSEI. *J. Clean. Prod.* **2021**, *302*, 126995. [CrossRef]
24. Gao, P.; Kasimu, A.; Zhao, Y.; Lin, B.; Chai, J.; Ruzi, T.; Zhao, H. Evaluation of the Temporal and Spatial Changes of Ecological Quality in the Hami Oasis Based on RSEI. *Sustainability* **2020**, *12*, 7716. [CrossRef]
25. Cao, J.; Wu, E.; Wu, S.; Fan, R.; Xu, L.; Ning, K.; Li, Y.; Lu, R.; Xu, X.; Zhang, J.; et al. Spatiotemporal Dynamics of Ecological Condition in Qinghai-Tibet Plateau Based on Remotely Sensed Ecological Index. *Remote Sens.* **2022**, *14*, 4234. [CrossRef]
26. Chen, Z.; Chen, J.; Zhou, C.; Li, Y. An ecological assessment process based on integrated remote sensing model: A case from Kaikukang-Walagan District, Greater Khingan Range, China. *Ecol. Inform.* **2022**, *70*, 101699. [CrossRef]
27. Qin, G.; Wang, N.; Wu, Y.; Zhang, Z.; Meng, Z.; Zhang, Y. Spatiotemporal variations in eco-environmental quality and responses to drought and human activities in the middle reaches of the Yellow River basin, China from 1990 to 2022. *Ecol. Inform.* **2024**, *81*, 102641. [CrossRef]
28. Liu, Y.; Xu, W.; Hong, Z.; Wang, L.; Ou, G.; Lu, N.; Dai, Q. Integrating three-dimensional greenness into RSEI improved the scientificity of ecological environment quality assessment for forest. *Ecol. Indic.* **2023**, *156*, 111092. [CrossRef]
29. Zheng, Z.; Wu, Z.; Chen, Y.; Guo, C.; Marinello, F. Instability of remote sensing based ecological index (RSEI) and its improvement for time series analysis. *Sci. Total Environ.* **2022**, *814*, 152595. [CrossRef]
30. Ning, L.; Jiayao, W.; Fen, Q. The improvement of ecological environment index model RSEI. *Arab. J. Geosci.* **2020**, *13*, 403. [CrossRef]
31. Yang, Y.; Li, H. Spatiotemporal dynamic decoupling states of eco-environmental quality and land-use carbon emissions: A case study of Qingdao City, China. *Ecol. Inform.* **2023**, *75*, 101992. [CrossRef]
32. Bhatti, M.I.; Do, H.Q. Recent development in copula and its applications to the energy, forestry and environmental sciences. *Int. J. Hydrogen Energy* **2019**, *44*, 19453–19473. [CrossRef]
33. Chen, L.; Guo, S. *Copulas and Its Application in Hydrology and Water Resources*; Springer: Singapore, 2019; pp. 99–108.
34. Wang, W.S.; Yang, H.B.; Huang, S.Z.; Wang, Z.M.; Liang, Q.H.; Chen, S.D. Trivariate copula functions for constructing a comprehensive atmosphere-land surface-hydrology drought index: A case study in the Yellow River basin. *J. Hydrol.* **2024**, *642*, 131784. [CrossRef]
35. Peng, S. *1-km Monthly Precipitation Dataset for China (1901–2022)*; National Tibetan Plateau/Third Pole Environment Data Center: Beijing, China, 2020. [CrossRef]
36. Mu, H.; Li, X.; Wen, Y.; Huang, J.; Du, P.; Su, W.; Miao, S.; Geng, M. A global record of annual terrestrial Human Footprint dataset from 2000 to 2018. *Sci. Data* **2022**, *9*, 176. [CrossRef] [PubMed]
37. Xu, X.; Liu, J.; Zhang, S.; Li, R. China Multi-Period Land Use Remote Sensing Monitoring Data Set (CNLUCC). 2018. Available online: http://www.resdc.cn (accessed on 15 September 2024). [CrossRef]
38. Wen, Q. Revision of Technical Specifications for Ecological Environment Condition Evaluation and its impact on the ecological evaluation process. *Environ. Prot. Circ. Econ.* **2016**, *36*, 69–71.
39. Mishra, N.B.; Crews, K.A.; Neeti, N.; Meyer, T.; Young, K.R. MODIS derived vegetation greenness trends in African Savanna: Deconstructing and localizing the role of changing moisture availability, fire regime and anthropogenic impact. *Remote Sens. Environ.* **2015**, *169*, 192–204. [CrossRef]
40. Lobser, S.E.; Cohen, W.B. MODIS tasselled cap: Land cover characteristics expressed through transformed MODIS data. *Int. J. Remote Sens.* **2007**, *28*, 5079–5101. [CrossRef]
41. Xu, H. A new index for delineating built-up land features in satellite imagery. *Int. J. Remote Sens.* **2008**, *29*, 4269–4276. [CrossRef]
42. Li, S.; Chen, X. A new bare-soil index for rapid mapping developing areas using LANDSAT 8 data. *Int. Arch. Photogramm. Remote Sens. Spat. Inf. Sci.* **2014**, *XL-4*, 139–144. [CrossRef]
43. Gringorten, I.I. A plotting rule for extreme probability paper. *J. Geophys. Res.* **1963**, *68*, 813–814. [CrossRef]
44. Abdi, H. The Kendall rank correlation coefficient. *Encycl. Meas. Stat.* **2007**, *2*, 508–510.
45. Sklar, M. Fonctions de répartition à n dimensions et leurs marges. *Ann. l'ISUP* **1959**, *8*, 229–231.
46. Genest, C.; Okhrin, O.; Bodnar, T. Copula modeling from Abe Sklar to the present day. *J. Multivar. Anal.* **2024**, *201*, 105278. [CrossRef]
47. Lourme, A.; Maurer, F. Testing the Gaussian and Student's t copulas in a risk management framework. *Econ. Model.* **2017**, *67*, 203–214. [CrossRef]
48. Hartmann, H.; Buchanan, H. Trends in Extreme Precipitation Events in the Indus River Basin and Flooding in Pakistan. *Atmos.-Ocean* **2014**, *52*, 77–91. [CrossRef]
49. Vazifehkhah, S.; Kahya, E. Hydrological and agricultural droughts assessment in a semi-arid basin: Inspecting the teleconnections of climate indices on a catchment scale. *Agric. Water Manag.* **2019**, *217*, 413–425. [CrossRef]
50. Runting, R.K.; Bryan, B.A.; Dee, L.E.; Maseyk, F.J.F.; Mandle, L.; Hamel, P.; Wilson, K.A.; Yetka, K.; Possingham, H.P.; Rhodes, J.R. Incorporating climate change into ecosystem service assessments and decisions: A review. *Glob. Chang. Biol.* **2017**, *23*, 28–41. [CrossRef]
51. Wang, H.; Liu, G.; Li, Z.; Zhang, L.; Wang, Z. Processes and driving forces for changing vegetation ecosystem services: Insights from the Shaanxi Province of China. *Ecol. Indic.* **2020**, *112*, 106105. [CrossRef]

52. Zhang, K.; Feng, R.; Zhang, Z.; Deng, C.; Zhang, H.; Liu, K. Exploring the Driving Factors of Remote Sensing Ecological Index Changes from the Perspective of Geospatial Differentiation: A Case Study of the Weihe River Basin, China. *Int. J. Environ. Res. Public Health* **2022**, *19*, 10930. [CrossRef]
53. Ju, X.F.; He, J.L.; Qi, Z.; Saitiniyazi, A. Evolution pattern and driving mechanism of eco-environmental quality in arid oasis belt—A case study of oasis core area in Kashgar Delta. *Ecol. Indic.* **2023**, *154*, 110866. [CrossRef]
54. Dong, Y.K.; Ma, W.; Tan, Z.W.; Wang, Y.; Zeng, W.J. Spatial and temporal variation of multiple eco-environmental indicators in Erhai Lake Basin of China under land use transitions. *Environ. Sci. Pollut. Res.* **2023**, *30*, 16236–16252. [CrossRef] [PubMed]
55. Yang, H.B.; Wu, Z.R.; Dawson, R.J.; Barr, S.; Ford, A.; Li, Y.F. Quantifying surface urban heat island variations and patterns: Comparison of two cities in three-stage dynamic rural-urban transition. *Sustain. Cities Soc.* **2024**, *109*, 105538. [CrossRef]
56. Fan, X.L.; Qu, Y.; Zhang, J.; Bai, E.D. China's vegetation restoration programs accelerated vegetation greening on the Loess Plateau. *Agric. For. Meteorol.* **2024**, *350*, 109994. [CrossRef]
57. Xu, D.; Bai, T.; Song, Y.; Xia, Z.; Duan, X.; Santamouris, M.; Cui, Y. Reassessing the climate mitigation potential of Chinese ecological restoration: The undiscovered potential of urban. *Innov. Geosci.* **2024**, *2*, 100068. [CrossRef]